

Investigation of Some Nonionic Surfactants as Corrosion Inhibitors for Carbon Steel in Sulfuric Acid Medium

Florina Branzoi^{1,*} and Viorel Branzoi²

¹ Institute of Physical Chemistry, 202 Splaiul Independenței, Bucharest, Romania,

² University Politehnica of Bucharest, 132 Calea Griviței, Bucharest, Romania,

*E-mail fbrinzoi@chimfiz.icf.ro

Received: 7 April 2017 / Accepted: 29 May 2017 / Published: 12 July 2017

Four nonionic surfactants have been investigated as corrosion inhibitors for carbon steel type OL37 in sulfuric acid solution by electrochemical methods, FT-IR spectroscopy and metallurgical microscopy techniques. The influence of inhibitor concentration on the corrosion rate, inhibition effectiveness and surface coverage was analyzed. Results indicate that these surfactants accomplish a great inhibiting action on carbon steel corrosion and acts that a mixed-type inhibitor. The inhibition effect of noionic surfactants may be due to either the adsorption of inhibitor molecules building a protective layer or the constitution of an insoluble complex of the inhibitor adsorption obeys the Langmuir model. The negative value of thermodynamic parameter like Gibbs free energy of adsorption ΔG_{ads}° indicates the spontaneity of adsorption process. Moreover, characterization utilizing FT-IR confirms the adsorption of inhibitors and the constitution of corrosion products on the carbon steel surface. EIS and potentiodynamic polarization results demonstrate its corrosion protection capacity.

Keywords: organic inhibitor, nonionic surfactant, carbon steel, potentiodynamic polarization, electrochemical impedance spectroscopy and FT-IR.

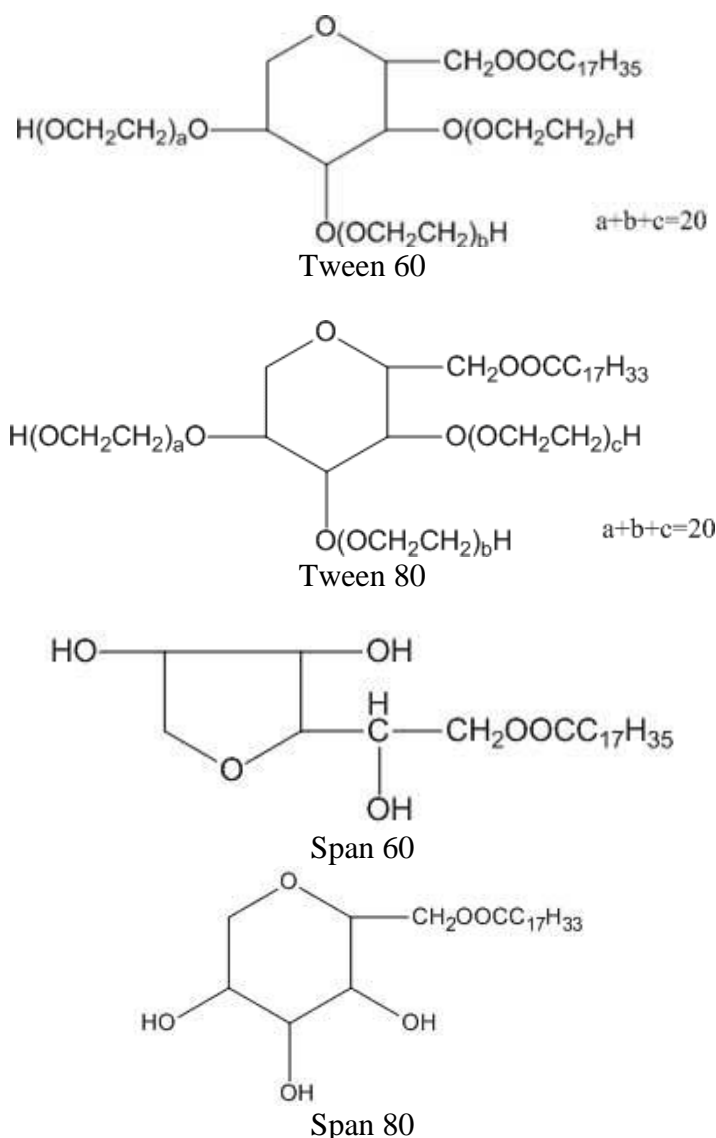
1. INTRODUCTION

Metals and alloys used in numerous industrial applications are sensitive to corrosion in various media. Carbon steel, the most widely used among them, is likewise very sensitive to corrosion, in particular in acidic environments [1-4]. Carbon steel is extensively used in numerous engineering applications (chemical processing, technological equipment, marine applications, petroleum production and refining) because of the mechanical property and low price [2-6]. It is susceptible to corrosion, mainly in acidic media because of its thermodynamic instability in aggressive environments.

The investigation of carbon steel corrosion phenomena became considerable especially in acidic environments for the increased industrial applications of acid solutions. The principal problem in utilizing carbon steel in aggressive environments is that of uniform corrosion [4-6]. Several techniques there are for improving the corrosion resistance of the carbon steel used in different domains. Treatment of the aggressive environment for the protection of metals and alloys can be obtained through elimination of the aggressive species or using of inhibitors. There are many techniques are used to improve the corrosion strength of the metallic materials used as mechanical parts in industry. The use of inhibitors, applying organic, metallic or inorganic coatings, cathodic and anodic protection, galvanostatic polymerization technique, nanostructured coating are methods for metal corrosion protection [7]. One of the optimal ways for corrosion inhibition is the use of the inhibitors. Some researches [2-3, 7-16] have related the inhibiting properties of alkyl amines, phenyl-alkyl amines, imines derivatives and various polymers as corrosion inhibitors. They check the corrosion action on the cathodic or anodic process or both. Since they usually influence the whole electrode surface, when they are showing enough concentration, they cannot be called anodic or cathodic inhibitors. Consequently, the corrosion mechanism and the corrosion inhibition of metals and its alloys in various aggressive environments have attracted the attention of a number of researches [2-3, 6-11]. It could be said, the corrosion protection properties of organic inhibitors is related with their adsorption properties [11-18]. Thus, the interaction of organic molecules and electrode surface can be demonstrated by adsorption isotherm and in general, inhibitors can act either by physical adsorption or chemisorption with the metal [17-25]. The influence of the adsorbed inhibitor is to protect the metal from the aggressive environment and/or to change the electrode processes that cause dissolution of the metal. It can be seen that, the adsorption depends especially on particular physico-chemical properties of the inhibitor molecule like as, functional groups, steric factors, aromaticity, electron density at the donor and π orbital character of donating electrons and also on the electronic structure of molecules [25-35]. In the main, organic inhibitors including polar groups with nitrogen, sulfur and oxygen and heterocyclic compounds with polar functional groups and/or conjugated double bond are considered as one of the efficient chemicals for the preventing the metals corrosion [32-39]. The surfactants are a vast category of organic inhibitors that were used for to obtain this protection [6, 35-40]. The ionic and nonionic surfactants were relevant to be great corrosion inhibitors for many metals and its alloy (iron, copper, aluminum, brass, zinc, magnesium and carbon steel). Numerous studies proposed that majority of surfactant inhibitors are adsorbed on the electrode surface by moving water molecules from the surface and obtaining a compact and consolidated barrier film. The capacity of a surfactant molecule to adsorb is mainly directly connected to its property to aggregate and to form micelles [3-6, 19, 37-40]. The aim of this study is to investigate the corrosion inhibition of carbon steel type OL 37 with four nonionic surfactants like Tween 60, Tween 80, Span 60 and Span 80 in sulfuric acid media. The inhibition properties of these nonionic surfactants on the carbon steel type OL37 has been analyzed by electrochemical methods, and the surface of carbon steel was studied by Fourier transform infrared spectroscopy (FT-IR) and by metallurgical microscopy methods. These surface analyses were achieved in order to verify the obtaining of a protective layer onto the electrode surface. Electrochemical methods are used to asses the anticorrosive properties of these new inhibitors.

2. EXPERIMENTAL

In this paper, the used organic inhibitors were some nonionic surfactants: Tween 60-polyoxyethylene sorbitan monostearate, Tween 80- polyoxyethylene sorbitan monooleate, Span 60-sorbitan monostearate and Span 80-sorbitan monooleate were from Aldrich products of pure quality (>97%). The concentrations of these surfactants were: 20, 50, 100, 300, 500, 800 and 1000 ppm. The aggressive medium has been 0.5M H₂SO₄ has been ready by dilution of AG 96% H₂SO₄ (from Merck) with bi-distilled water. All chemicals were reagent grade and used as received without further purification.



Scheme 1. Chemical structure of the nonionic surfactants used

Experiments were performed on carbon steel type OL 37 electrode with composition: C% 0.15; Si% 0.09; Mn% 0.4; P% 0.023; S% 0.02; Al% 0.022; Ni% 0.001; Cr% 0.001; Fe% 99.293. Corrosion tests were accomplished with and without of various concentrations of nonionic surfactants. The working electrode has been OL 37 in the form cylindrical with a surface area of 0.5 cm². The

cylindrical form is favorite, as it ensures a higher surface and without edges. The OL 37 electrode has been polished with emery papers of varied granulation (600, 1200, 2500, 4000 grid) up to mirror-luster. Afterwards, the carbon steel electrode has been washed with bi-distilled water and introduced in the electrochemical cell. Each experiment there has been realized at temperature of 25°C under atmospheric condition. The polarization compartment of OL 37 in 0.5 M H₂SO₄ with and without of nonionic surfactants has been analyzed by potentiostatic and potentiodynamic techniques. Experimental methods were described previously [2, 5, 35]. For all measurements the electrochemical polarizations have been started on 30 minutes after the working electrode was put into aggressive solution, to allow the stabilization of the stationary potential. The working electrode potential has been constantly measured with reference to the (SCE) and has been plotted against current from external circuit, obtaining the anodic or cathodic curves according to the variation of the working electrode potential [2, 3, 6, 7, 35]. Quasi steady-state polarization curves have been obtained by scanning the working electrode potential in anodic and cathodic direction from E_{corr} (±250mV by E_{corr}) at the rate of 2mVs⁻¹ [2, 3, 7, 35]. The inhibiting activity has been analyzed by drawing the polarization curves achieved by potentiodynamic technique, calculation of the kinetic parameters of corrosion in situation of solutions with various concentrations of inhibitors, mainly the corrosion current densities, and their comparison with the kinetic parameters of the solution without inhibitors. Analysis of Tafel polarization curves has been realized by scanning the potential from cathodic to anodic potentials at a sweep of 2mVs⁻¹ in the potential domain from -900mv to -150mV versus to OCP-open circuit potential. Electrochemical impedance spectroscopy measurements have been realized in a frequency domain from 100KHz to 40mHz at potentiodynamic condition with an AC wave of ± 10 mV (peak-to-peak) at corrosion potential (E_{corr}) [2, 3, 7, 35]. The determinations have been repeated with every solution until a good reproducibility of the dates has been realized. Electrochemical polarization curves and electrochemical impedance spectroscopy tests have been performed out by using a single – compartment cell with the conventional three electrode set up at temperature 25⁰C. The electrochemical cell has been related to a VoltaLab potentiostat coupled to a PC running VoltaMaster software. A saturated calomel electrode (SCE) has been realized like the reference electrode and a bright platinum gauze as an auxiliary electrode. The working electrode has been a carbon steel of type OL 37 with a surface area 0.5 cm² [2, 3, 7, 35]. The electrochemical experiments (potentiostatic, potentiodynamic and the electrochemical impedance spectroscopy technique) have been realized utilizing VoltaLab PGZ 301 instrument Potentiostat/Galvanostat. Surface analysis on the OL 37 sample of the adsorbed film has been examined by FTIR spectroscopy (FTIR spectrometer Tensor 37 Bruker optik) and metallographic micrographies (Microscope Hund H660).

3. RESULTS AND DISCUSSION

3.1. Potentiodynamic polarization

Figure 1 shows the typical potentiodynamic polarization curves of OL37 carbon steel electrode in 0.5M H₂SO₄ medium with and without of different concentrations of four nonionic surfactants:

Tween 60, Tween 80, Span 60 and Span 80. It can be seen from figure 1 that both cathodic and anodic current densities decrease when the organic inhibitors is added in the aggressive solution, and the variations of anodic and cathodic current densities with inhibitor concentrations are more evident. This fact indicates that the inhibitors repressed of the anodic and cathodic reactions. This fact may be due the presence in their molecules of the groups with different affinity with the solvent, such as of the hydrocarbonate hydrophobic groups and hydrophilic nonionic groups, offers them tensioactive and colloidal properties [6].

The addition of four nonionic surfactants led in all the cases to protection of the corrosion process in acidic medium. Also, the inhibition effectiveness increases with the hydrophobic chain length molecule and the utilized concentration of the inhibitor. At a concentrations higher than the CMC, the inhibiting action of these inhibitors increases rapidly [6] Also, in figure 1 we observed for both the anodic metal dissolution and cathodic hydrogen evolution processes have been inhibited by the addition of these nonionic surfactants to the corrosive environment [6].

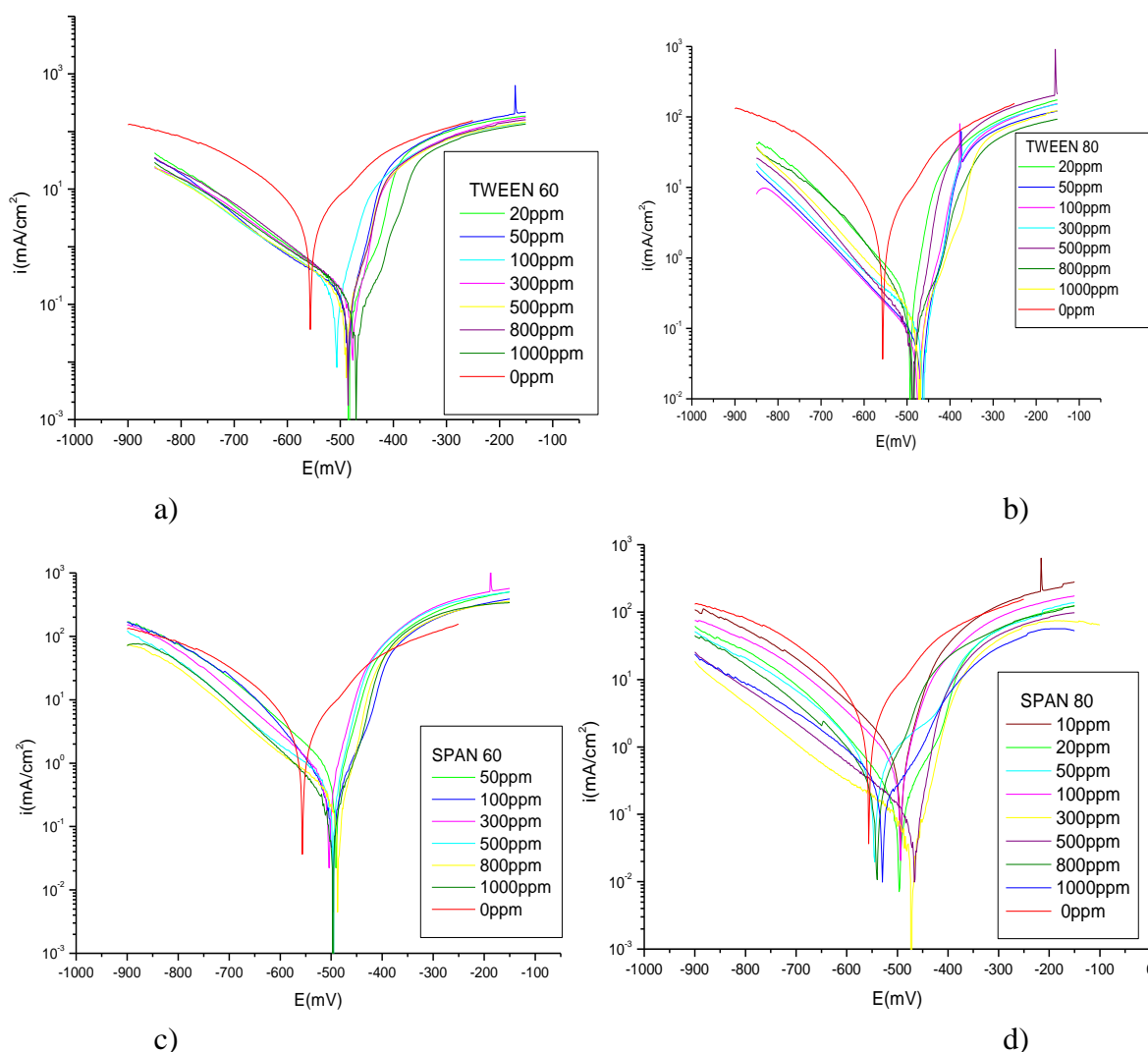


Figure 1. Polarization curves for the carbon steel OL 37 in 0.5M H₂SO₄ with and without for various concentrations of inhibitor a) Tween 60, b) Tween 80, c) Span 60 and d)Span 80 in the domain potential from -900mV to -150mV at E_{corr} at a sweep rate of 2mVs⁻¹ and at 25⁰C

The inhibitions of these reactions are more accentuated with the increasing inhibitor concentration while the corrosion potential values displacement the more positive values.

Electrochemical corrosion parameters, i.e. corrosion current density, cathodic and anodic Tafel slopes and corrosion potential, achieved of the Tafel extrapolation of the polarization curves have been presented in Tables 1-4, where the inhibition efficiency were calculate [28]. The existence of inhibitor determines a significant decrease in corrosion rate; change the anodic curves to more positive potentials and the cathodic curves to more negative potentials. This fact can be attributed to adsorption of inhibitor on the electrode surface.

Examination of the polarization curves by figure 1 show that at low overvoltages, the Tafel relation is verified, indicating that the anodic and cathodic processes are activation-controlled [2, 3, 6, 35]. At bigger overvoltages a limiting current display on the anodic and cathodic polarization curves indicating that, the transport of ions to the electrode surface becomes the rate-determining step - concentration polarization [6]. The addition of Tween 60, Tween 80, Span 60 and Span 80 decreases the corrosion current density (i_{corr}) values significantly for all the analyzed concentrations due to increase in blocked fraction of the electrode surface by adsorption. This shows that these surfactants act like a mixed inhibitor. The adsorption of the nonionic surfactant molecules over the OL 37 surface decreases the interaction from the electrode surface and the aggressive ions (SO_4^{2-}) which intensively decreases the corrosion process and increases their inhibitive effect. Surfactants congregate in special mode at the interface metal/electrolyte and change the interfaces and so, check, decrease or hinder reactions from a layer and its environment, when introduced in the environment. We are assuming that the corrosion protection of the electrode with the obtaining of a protective film of adsorbed species at the OL 37 surface. The inhibition effect of these inhibitors has been accomplished by supposing that the process of inhibition by surfactant molecules is chemisorption and physical adsorption. The inhibitors of Tween 60, Tween 80 exhibited more corrosion inhibition of OL37 in acidic media than Span 60 and Span 80 inhibitors in same conditions as demonstrated by the data presented in Tables 1-4 and figure 1.

Table 1. Electrochemical parameters of OL 37 in 0.5M H₂SO₄ at various concentrations of Tween 60 at temperature of 25°C

Concentration (ppm)	i_{corr} (mAcm ⁻²)	R_p Ωcm ⁻²	R_{mpy}	$P_{mm/year}$	K_g g/m ² h	E (%)	-E _{corr} (mV)	b_a (mVdec ⁻¹)	$-b_c$ (mVdec ⁻¹)	θ
0	1.10	10.16	513.33	13.02	11.66	-	556	101	83	
20	0.069	105	32.2	0.817	0.732	93	487	45	73	0.93
50	0.056	122	26.13	0.663	0.593	92	488	46	66	0.92
100	0.087	77	40.6	1.03	0.92	91	510	42	57	0.91
300	0.036	124	16.8	0.426	0.381	96	478	40	48	0.96
500	0.037	122	17.26	0.438	0.392	96	492	54	61	0.96
800	0.045	114	21	0.532	0.477	95	488	40	54	0.95
1000	0.046	112	21.46	0.544	0.487	95	473	48	64	0.95

Table 2. Electrochemical parameters of OL 37 in 0.5M H₂SO₄ at various concentrations of Tween 80 at temperature of 25°C

Concentration (ppm)	i_{corr} (mAcm ⁻²)	R_p Ωcm ⁻²	R_{mpy}	$P_{mm/year}$	K_g g/m ² h	E (%)	-E _{corr} (mV)	b_a (mVdec ⁻¹)	$-b_c$ (mVdec ⁻¹)	θ
0	1.10	10.16	513.33	13.02	11.66	-	556	101	83	
20	0.144	48	67.2	1.705	1.522	87	493	40	74	0.87
50	0.061	212	28.46	0.741	0.647	94	467	56	137	0.94
100	0.06	207	28	0.710	0.636	94	478	54	132	0.94
300	0.0521	146	24.26	0.615	0.551	95	465	42	80	0.95
500	0.039	152	18.2	0.461	0.413	96	487	38	54	0.96
800	0.09	123	42	1.065	0.954	92	488	68	75	0.92
1000	0.099	123	46.2	1.172	1.051	91	475	73	115	0.91

Table 3. Electrochemical parameters of OL 37 in 0.5M H₂SO₄ at various concentrations of Span 60 at temperature of 25°C

Concentration (ppm)	i_{corr} (mAcm ⁻²)	R_p Ωcm ⁻²	R_{mpy}	$P_{mm/year}$	K_g g/m ² h	E (%)	-E _{corr} (mV)	b_a (mVdec ⁻¹)	$-b_c$ (mVdec ⁻¹)	θ
0	1.10	10.16	513.33	13.02	11.66	-	556	101	83	
50	0.369	34	172.2	4.37	3.91	77	505	47	63	0.77
100	0.305	38	142.33	3.612	3.234	72	494	53	77	0.72
300	0.242	41	112.93	2.866	2.566	78	499	56	79	0.78
500	0.126	57	58.8	1.492	1.33	88	501	55	75	0.88
800	0.08	79	37.33	0.947	0.848	92	489	44	60	0.92
1000	0.231	47	107.8	2.736	2.45	79	496	50	84	0.79

Table 4. Electrochemical parameters of OL 37 in 0.5M H₂SO₄ at various concentrations of Span 80 at temperature of 25°C

Concentration (ppm)	i_{corr} (mAcm ⁻²)	R_p Ωcm ⁻²	R_{mpy}	$P_{mm/year}$	K_g g/m ² h	E (%)	-E _{corr} (mV)	b_a (mVdec ⁻¹)	$-b_c$ (mVdec ⁻¹)	θ
0	1.10	10.16	513.33	13.02	11.66	-	556	101	83	
20	0.131	108	61.13	1.551	1.389	88	496	74	93	0.88
50	0.301	44	140.46	3.601	3.192	72	546	96	88	0.72
100	0.332	32	154.93	3.932	3.521	70	494	50	113	0.70
300	0.015	281	7.18	0.182	0.163	97	472	44	53	0.97
500	0.035	197	16.33	0.414	0.371	96	466	52	69	0.96
800	0.121	93	56.46	1.433	1.283	89	541	62	79	0.89
1000	0.197	75	91.93	2.33	2.089	82	532	90	71	0.82

The surfactants Tween (60 and 80) have a bigger protection effect and the lowest corrosion current density than the inhibitors Span(60 and 80), because the Tween of surfactants are polyoxyethylene derivatives of Span product and these polyoxyethylene derivatives increases the anticorrosive properties of carbon steel surface by preventing the penetration of aggressive ions. The inhibition properties of Tween 60 and Tween 80 surfactants possibly assigned to the presence of

electron rich of the nonionic polyoxyethylene chains. The corrosion inhibition is proved by the occurrence that the hydrocarbonate chains with polyoxyethylene derivatives competitively adsorb onto the OL 37 surface blocking the active sites and consequently the SO_4^{2-} anion is hindered from reaching the OL37 surface and anticorrosion protection is realized [6, 7, 35].

The examination of figure 1 and Tables 1-4 revealed that the corrosion rate have been significantly decreased in inhibited solutions when in comparison with the aggressive environment and to increase of the inhibition performance. By analyzing in comparison the inhibition efficiency and the corrosion rate (R_{mpy} , in mil per year; P, in mm per year and Kg, in $\text{gm}^{-2}\text{h}^{-1}$) for all four inhibitors, in the identical condition, one can observe as, the Tween 60 and Tween 80 have an excellent effectiveness for anticorrosion protection of OL 37 in 0.5M H_2SO_4 and Span 60 and Span 80 have a good inhibition efficiency. The best effectiveness is realized at the inhibitor concentration for Tween 60 is 500ppm and 300ppm, for Tween 80 is 300ppm and 500ppm, for Span 60 is 800ppm and 1000ppm, and for Span 80 is 800ppm and 500ppm. These results demonstrate that these nonionic surfactants can be considered as mixed type corrosion inhibitors. The dates obtained in this investigation could be explained by the effects of surfactants on the electrochemical properties of -OL 37 electrode.

3.2. Electrochemical Impedance Spectroscopy (EIS)

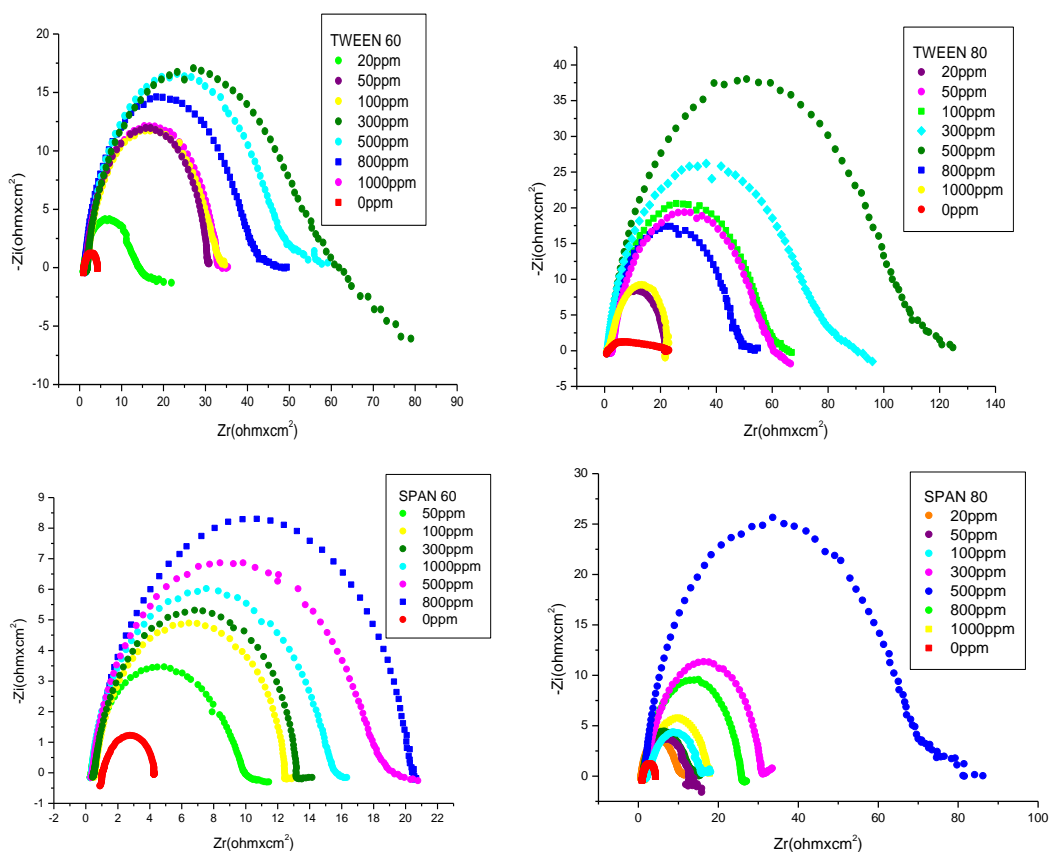


Figure 2. The Nyquist plot of OL 37 in 0.5M H_2SO_4 at various inhibitor concentrations: Tween 60, Tween 80, Span 60 and Span 80 at the corrosion potential (E_{corr}) and at temperature 25°C

The corrosion inhibition influence of four nonionic surfactants on OL 37 was also studied by EIS. Impedance tests have been achieved at open circuit potential on the frequency domain from 100 kHz to 40 mHz with an AC wave of ± 10 mV (peak-to-peak) and the impedance results have been realized at a rate of 10 points per decade change in frequency[2, 7, 35]. Figure 2 indicates the Nyquist graph of OL 37 in 0.5M H₂SO₄ medium with and without of these inhibitors at different concentrations.

The impedance spectra of carbon steel electrode show one capacitive loop. The size of capacitive loop in the inhibited solution is greater than that in the corrosive medium. In all cases, it is found that the diameter of the semicircle increases with increasing concentration of these inhibitors (Tween 60, Tween 80, Span 60 and Span 80), ensuring that the formed protective layer has been accomplished by the addition of these inhibitors. In the main, the single capacitive loop as presented in the Nyquist plots assume one time constant most likely associated with the charge transfer process. Moreover, these capacitive loops are not perfect semicircles and this fact is assigned at frequency dispersion, largely attributed to roughness and inhomogeneities of the electrode surface [2, 7, 35]. The semicircular shape reveals that the corrosion of OL 37 is checked by charge transfer and the existence of surfactant does not modification the process of dissolution.

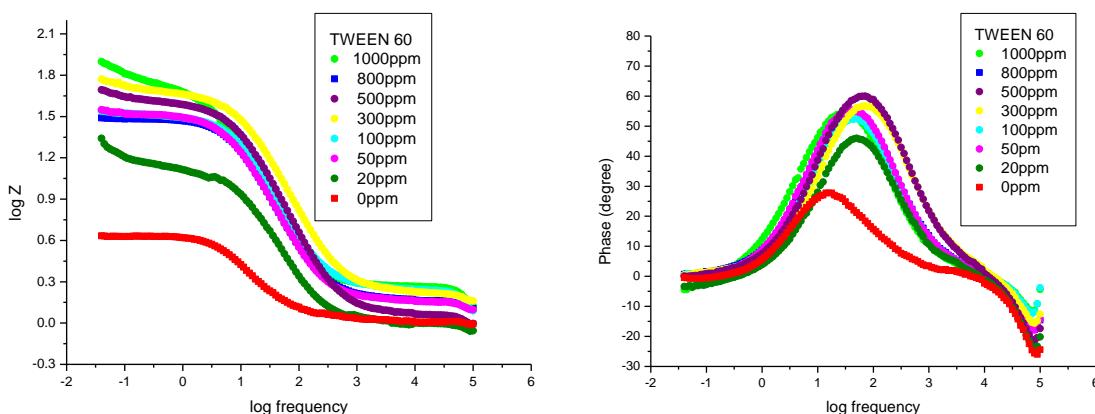


Figure 3. The Bode plot of OL 37 in 0.5M H₂SO₄ at various concentrations inhibitor Tween 60 at 25⁰C

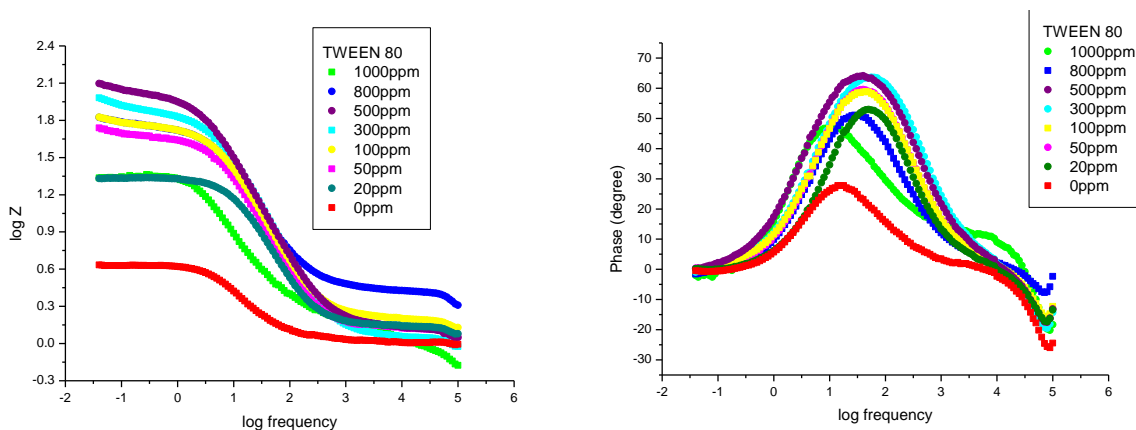


Figure 4. The Bode plot of OL 37 in 0.5M H₂SO₄ at various concentrations inhibitor Tween 80 at 25⁰C

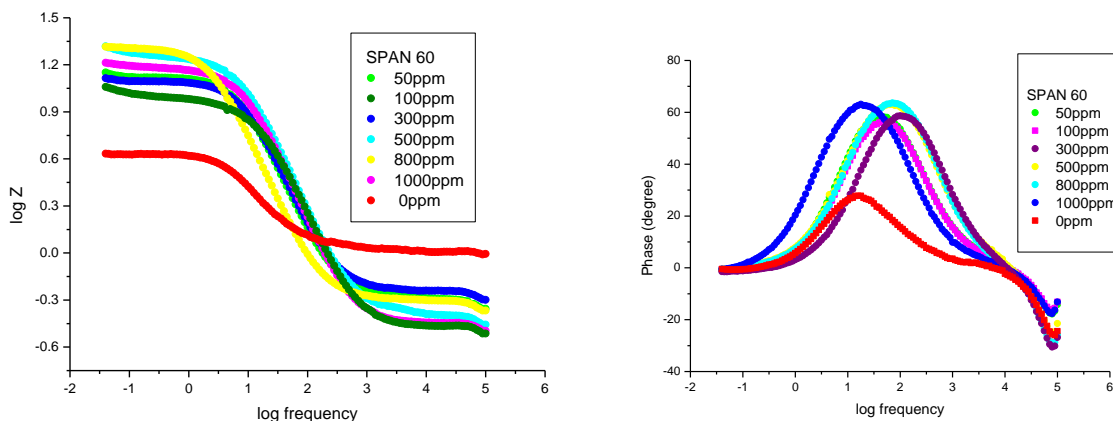


Figure 5. The Bode plot of OL 37 in 0.5M H₂SO₄ at various concentrations inhibitor Span 60 at 25⁰C

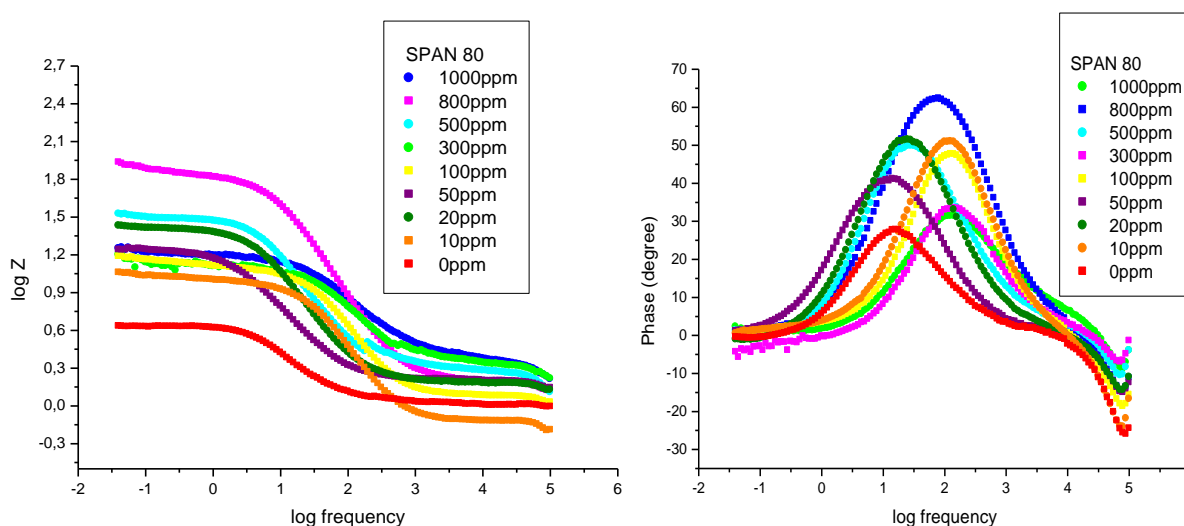


Figure 6. The Bode plot of OL 37 in 0.5M H₂SO₄ at various concentrations inhibitor Span 80 at 25⁰C

Figure 2 as well shows that the diameters of these semicircles in the presence of 300ppm and 500ppm Tween 60, 500ppm Tween 80, 800ppm Span 60 and for 500ppm Span 80 are much higher than those in the absence of organic compounds, resulting that has good anticorrosion protection onto the OL 37 in 0.5M H₂SO₄ solution.

Bode graphs exhibited in Figures 3-6 are in agreement with Nyquist plots (figure 2). It can be said that without of surfactant the OL 37 indicate one time constant according to a phase angle of 30° at average and low frequencies this presents an inductive compartment with low diffusive trend.

From figures 3-6, it can be said that with the inhibitor on the graph-phase angle in according on the frequency logarithm exhibits a maximum very well determined attributed at a phase angle of appreciative of 70° therefore, in this case the electrode has a greater capacitive behaviour, in concordance with the Nyquist plots [7]. The electrochemical impedance spectra for all these nonionic surfactants in the studied concentration interval are presented by one deformed semicircle, with a great frequency capacity loop and low frequency inductive loop. Variation from ideal circular form, frequently is characterized like frequency dispersion has been assigned to surface inhomogeneities and

roughness of the metal surface due to corrosion [11, 35, 39-44] They have been fitted utilizing one time constant equivalent mode with capacitance (C), the charge transfer resistance (R_{ct}) and R_s is solution resistance [2]. The double layer capacitance (C_{dl}) values decreases once with the increasing of the surfactant concentration and achieves very low values for the best concentrations of inhibitors for all the analyzed processes which showing that the diminishing of charges accumulated in the double layer due to the obtaining of adsorbed surfactant film. This fact shows once more that these surfactants provide best corrosion protection. Similar results were reported in several studies [2, 7, 35, 39-45]. The equivalent circuit used in this paper is shown in Figure 7.

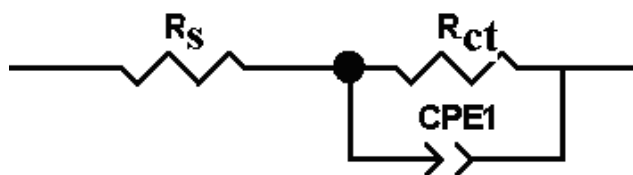


Figure 7. Equivalent circuit

3.3. Effect of temperature

The influence of temperature on the inhibitory effect of the nonionic surfactants at a concentration of 500ppm for carbon steel OL 37 in 0.5M H_2SO_4 at 298, 308, 318 and 328 $^{\circ}K$ has been analyzed by potentiodynamic polarization method. It can be said that, the corrosion rate increased with increasing temperature in inhibited and uninhibited solutions. The inhibition effect of these inhibitors decrease with increasing temperature, while the corrosion protection of OL 37 in H_2SO_4 medium in presence of these surfactants is realized by the adsorption of inhibitor, however, at greater temperature determine the desorption of these nonionic surfactants molecules from the electrode surface.

The dependency of corrosion rate on temperature can be related by the Arrhenius equation and transition equation [42-46]

$$i_{corr} = A \exp\left(\frac{-E_a}{RT}\right);$$

$$i_{corr} = \frac{RT}{Nh} \exp\left(\frac{\Delta S_a^*}{R}\right) \exp\left(\frac{\Delta H_a^*}{RT}\right)$$

where i_{corr} is the reaction rate, A is a pre-exponential factor, E_a the apparent activation energy of OL 37 dissolution process, R the universal gas constant and T the absolute temperature, ΔH_a^* the apparent enthalpy of activation, ΔS_a^* the apparent entropy of activation, h Planck' constant, N the Avogadro number. Figure 8a represented the Arrhenius plot, corrosion rate against of $1/T$ for carbon steel OL 37 in 0.5M H_2SO_4 in presence and absence of four nonionic surfactants. The plots achieved are straight lines and slope of each straight line gives activation energy. The negative slope of activation energy shows the adsorption of these nonionic surfactants on the carbon steel surface. Figure 8b show a graph of logarithm corrosion rate/T versus of $1/T$. Straight lines are achieved with a slope of $(-\Delta H^*/R)$ and an intercept of $(\ln(R/Nh)+(\Delta S^*/R))$, from which the values ΔH^* and ΔS^* were calculated

(see table 5). In this work, the data of E_a with these nonionic surfactants are greater than the uninhibited solution and these data are presented in table 5.

Table 5. The values of E_a , ΔH^0 and ΔS^0 for four nonionic surfactants in 0.5M H_2SO_4

Inhibitor	E_a (KJ/mol K)	ΔH^0 (KJ/mol K)	ΔS^0 (J/mol K)
Tween 60	62.258	59.77	-71.645
Tween 80	54.347	57.3	-73.088
Span 60	51.572	44.11	-111
Span 80	52.178	44.28	-95.25
H_2SO_4	46.43	34.24	-131.31

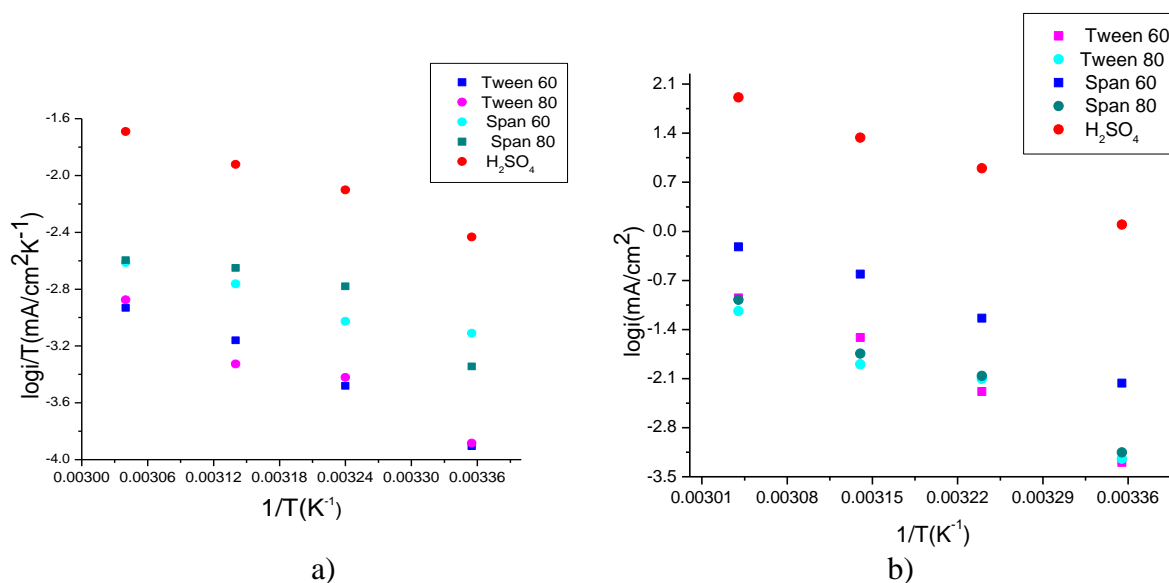


Figure 8. Arrhenius plot for OL 37 in 0.5M H_2SO_4 with and without of Tween 60, Tween 80, Span 60 and Span 80 at a concentration of 500ppm at 298, 308, 318 and 328 0K

The greater increase in the activation energy of the corrosion process with these inhibitors indicates the greater protection effect of these nonionic surfactants, which indicated physical adsorption, the energy barrier for the corrosion process increases and the surfactant molecules adsorption on the OL 37 surface which decreases the interaction from the aggressive environment and the electrode surface. Also, the increase in activation energy in presence of these four inhibitors in the 0.5M H_2SO_4 medium shows that physical adsorption appears in the first stage. From another point view, the adsorption process of an inhibitor molecule is not considered only as a physical or as

chemical adsorption process, likewise, from adsorption experimental data it can be concluded we have a mixed type of adsorption: physisorption and chemisorption of the surfactants on the electrode surface. The greater E_a value in the inhibited solution is interpreted with the increases thickness of the double layer which improves the activation energy of the corrosion reaction [43-47].

3.4. Adsorption isotherms

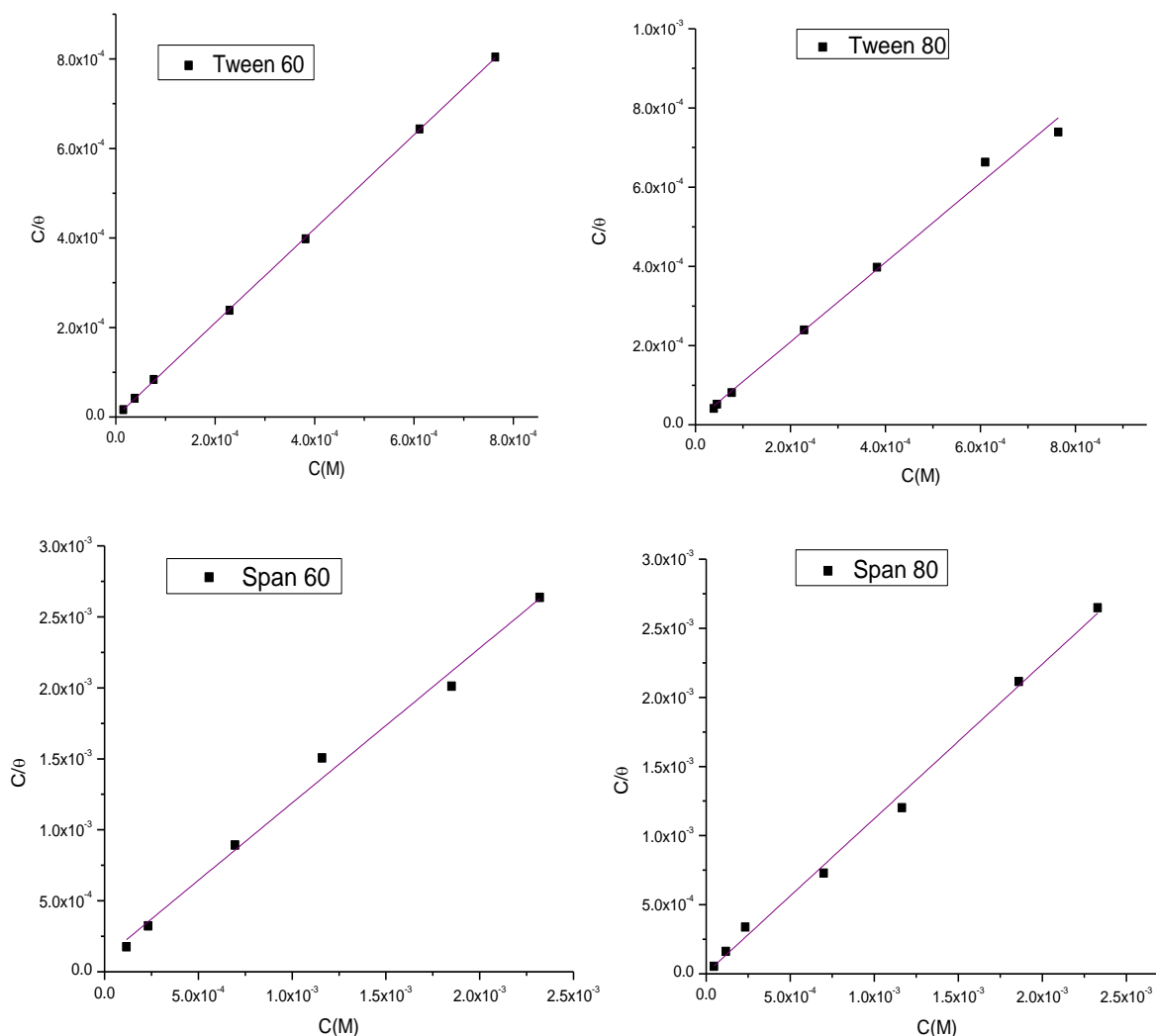


Figure 9. Langmuir plot for (a) Tween 60, (b) Tween 80 (c) Span 60 and d) Span 80 on OL 37 in 0.5M H_2SO_4 at various inhibitor concentrations

Adsorption isotherm is very significant in obtaining the mechanism of organo-electrochemical processes. As well, the highest inhibition effectiveness is an effect of the adsorption process. The adsorption isotherm can offer significant knowledge on the interaction of surfactant and electrode surface. To measure the influence of surfactant concentration on the corrosion rate, it is used to match the rate values to equilibrium adsorption relations, as Langmuir equation [6-7, 35, 42-49]: $\theta/(1-\theta) = KC$, where θ is the degree of the coverage on the electrode surface by the inhibitor and K is the equilibrium constant of the adsorption process, θ is determined by: $\theta = (i_{corr} - i_{inh})/i_{corr}$ where i_{inh} and i_{corr}

are the corrosion current density in 0.5M H₂SO₄ with and without inhibitor. All correlation coefficient (R^2) exceeded 0.99 (Tween 60 $R^2=0.9999$; Tween 80 - $R^2=0.9995$; Span 60 $R^2=0.9954$ and Span 80 $R^2=0.9965$) presents that the protection has been assigned to adsorption of these surfactants on the electrode surface. Utilization of the Langmuir behavior is frequently demonstrated with the argument that protection shall include adsorption. The reaction from the first step of the corrosion process of OL 37 in 0.5M H₂SO₄ in presence of inhibitors is: $Fe + INH \leftrightarrow Fe(INH)_{ads} \leftrightarrow Fe^{n+} + ne^- + INH$. When, we have a high inhibitor concentration, a compact and coherent layer is obtained onto OL 37 electrode surface that reduced aggressive attacks onto the metal.

In this study, straight lines have been achieved when concentration C_{inh}/θ were plotted versus C_{inh} . with a slope of unity. The linear relationship suggests that the adsorption of surfactants obeys the Langmuir adsorption isotherm (Figure 9). The great date of the adsorption equilibrium constant considers the great adsorption capacity of this inhibitor onto OL 37 surface.

The equilibrium constant of the adsorption process (K_{ads}) is reported by the standard adsorption free energy (ΔG_{ads}°) obtained by the relation: $\ln K_{ads} = -(\Delta G_{ads}^{\circ} / RT)$ [6-7, 35, 45-49].

The deduced value of ΔG_{ads}° obtained is negative and represents that the adsorption of organic inhibitor is a spontaneous reaction, and moreover the negative data of ΔG_{ads}° likewise indicate the strong interaction of the surfactant molecule with the surface.

The obtained values ΔG_{ads}° around -20KJmol^{-1} or smaller presents the electrostatic interaction from charged metal surface to charged in the bulk of the solution while those around -40KJmol^{-1} or higher imply charge sharing or charge transfer between the electrode surface and organic molecules (see Table 6) [2, 6-7, 11, 35, 40-49].

Table 6. The values of K_{ads} and ΔG_{ads}° for the nonionic surfactants in 0.5M H₂SO₄

The system	K_{ads}, M^{-1}	$\Delta G_{ads}^{\circ} \text{ KJmol}^{-1}$	The adsorption
Tween 60 +0.5M H ₂ SO ₄	11.34×10^4	-35.524	Chemisorption and Physical adsorption
Tween 80 +0.5M H ₂ SO ₄	16.98×10^5	-35.422	Chemisorption and Physical adsorption
Span 60 +0.5M H ₂ SO ₄	1.01×10^4	-22.833	Physical adsorption
Span 80 +0.5M H ₂ SO ₄	21.338×10^4	-30.387	Physical adsorption and Chemisorption

The inhibition effect examination of these surfactants has been achieved by supposing that the mechanism of protection by organic molecules can be realized by two modes of interaction: physical adsorption and chemisorption.

Mechanism of inhibition can be explained from the results obtained, it has been concluded that all the organic inhibitors (Tween 60, Tween 80, Span 60 and Span 80) prevent the corrosion of OL 37 in 0.5M H₂SO₄ by adsorption of inhibitors at metal/medium interface. Adsorption of these surfactants can be reached by physical adsorption and chemisorption process. This process is affected by the

nature and charge of the metal, the chemical composition of the inhibitor and the type of electrolyte [48-51]. The inhibition effectiveness of these surfactants against the corrosion OL 37 in 0.5M H₂SO₄ can be interpreted on the based on the number of adsorption sites, molecular dimension and the way of interaction with the electrode surface, the interaction from unshared electron pairs of the oxygen atoms in the polyoxyethylene chains and the free d-orbital of Fe surface atom[19, 49-52]. Physical adsorption needs existence of both electrically charged surface of the metal and charged species in the majority of the medium and the chemisorption process assume charge sharing or charge transfer from the surfactant molecules to the electrode surface to obtain a coordinate bond [48-52].

3.5. Surface analysis by FTIR spectrum

Fourier transform infrared (FT-IR see figures 10-13) spectra were accomplished with a Bruker optics spectrometer at room temperature. All spectra in this work were obtained at a resolution 4cm⁻¹ in the region 4000-650cm⁻¹ [2, 7, 35]

In this study, FT-IR spectra revealed that the surfactants were adsorbed on the electrode surface. FT-IR spectrum is a technique to determine the type of functional groups of organic compounds adsorbed on the metal surface, and can be utilized also to identify the nature of the bonding [2, 7, 35, 51-53]. In order to analyze the protective film obtained on the metal surface with four surfactants on the OL 37 surface has been analyzed by FT-IR spectra.

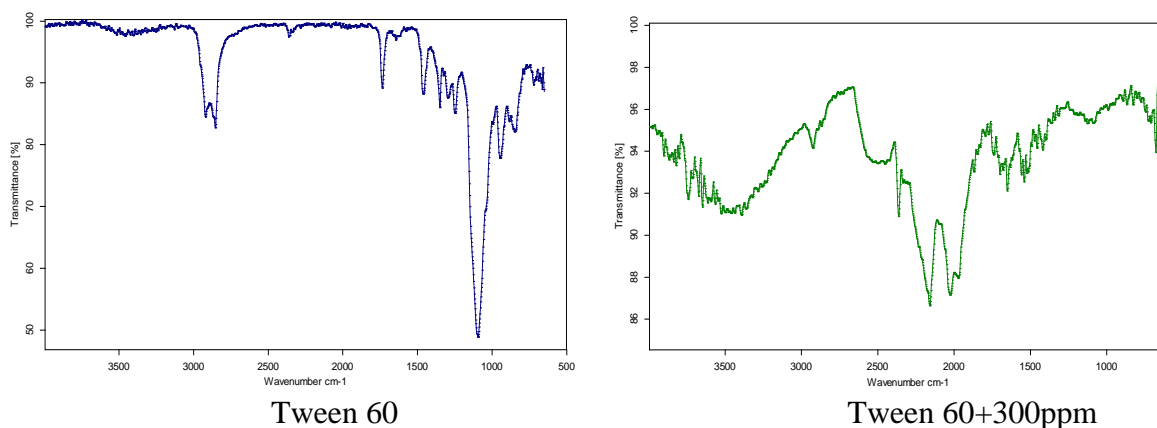


Figure 10. FT-IR transmittance spectrum of (a) Tween 60 and (b) OL37+300 ppm Tween 60

The FT-IR spectrum of Tween 60 is show in Figure 10a and the FT-IR spectra of adsorbed protective film obtained on the electrode after immersion in aggressive solution including optimum concentration of surfactant 300ppm Tween 60 is indicated in Figure 10b. It can be observed all significant peaks of nonionic surfactant-Tween 60 shown up in adsorption film on the electrode surface. The band at 3363 cm⁻¹ is ascribed to O-H stretching.

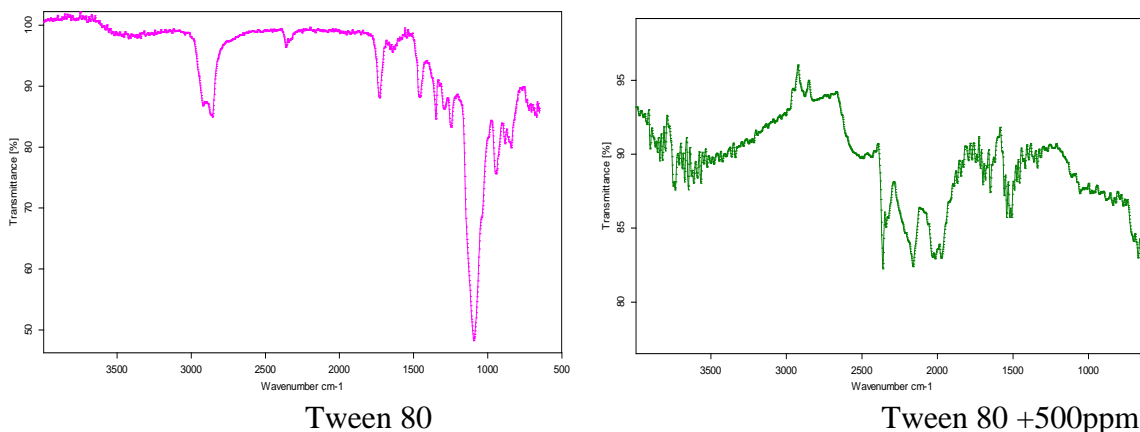


Figure 11. FT-IR transmittance spectrum of (a) Tween 80 and (b) OL37+500 ppm Tween 80

The peak around 2920 and 2857 cm^{-1} are attributed to the aliphatic $-\text{CH}_2$ symmetric and asymmetric stretching vibration and that at 1736 cm^{-1} to $\text{C}=\text{O}$. The peaks at 1658 and 1462 cm^{-1} ascribed to the vibration of O heterocycling ring. The existence of C-H and C-O-C is determined by their stretching modes at 1350 and 940 cm^{-1} . The characteristic peaks at 1339 correspond to the C-H bending in $-\text{CH}_2$, $-\text{CH}_3$. The band at $1100\text{--}800\text{ cm}^{-1}$ is assigned to C-O-C vibration in $(\text{CH}_2\text{CH}_2\text{O})$. Furthermore, these FT-IR techniques shown up at 3832 cm^{-1} the direct bonding from Fe atoms and Tween 60 molecules via O atoms and the obtaining Fe-inhibitor complex and this establishes that there is just chemical adsorption realized onto the surface of OL37 [2, 7, 35, 51-54]. Comparing figures 10a and 10b, it can be suggested that Tween 60 is adsorbed on the electrode surface. This is already confirmed from the Langmuir adsorption isotherm studies.

FT-IR transmittance spectrum of surfactant Tween 80 is depicted in Figure 11a. From figure 11a, a broad peak at 3412 cm^{-1} show the existence of the OH group. The band at $2924\text{--}2857\text{ cm}^{-1}$ is ascribed to the aliphatic CH_2 symmetric and asymmetric stretching vibration. The presence of $\text{C}=\text{O}$ stretching ways can be manifest in the domain 1729 cm^{-1} . The band at 1326 to 1247 cm^{-1} respectively is attributed to C-H bending and the peak at 1095 cm^{-1} is assigned of C-O-C in $(\text{CH}_2\text{CH}_2\text{O})_n$. The FT-IR transmittance spectrum achieved for the OL 37 with 500ppm Tween 80 surfactant is indicated in Figure 11b. This presents the characteristic band for the adsorbed Tween 80 on the electrode surface. A broad band in the domain from 3341 cm^{-1} is ascribed to O-H stretching, the existence of the peak in range 1520 cm^{-1} is for OH bending. The peaks for $\text{O}=\text{C}-\text{O}$ stretching ways can be attributed in the domain $2900\text{--}2800\text{ cm}^{-1}$ and the band at 1723 cm^{-1} is assigned to $\text{C}=\text{O}$. The bands at 1200 cm^{-1} and 1090 cm^{-1} are ascribed to CH_2 and C-O-C stretching vibration. The bands 3854 cm^{-1} and 3730 cm^{-1} are assigned to Fe-O bending [2, 7, 35, 51-55]. Comparing figures 11a and 11b, it can be considered that Tween 80 is adsorbed on the OL 37 surface.

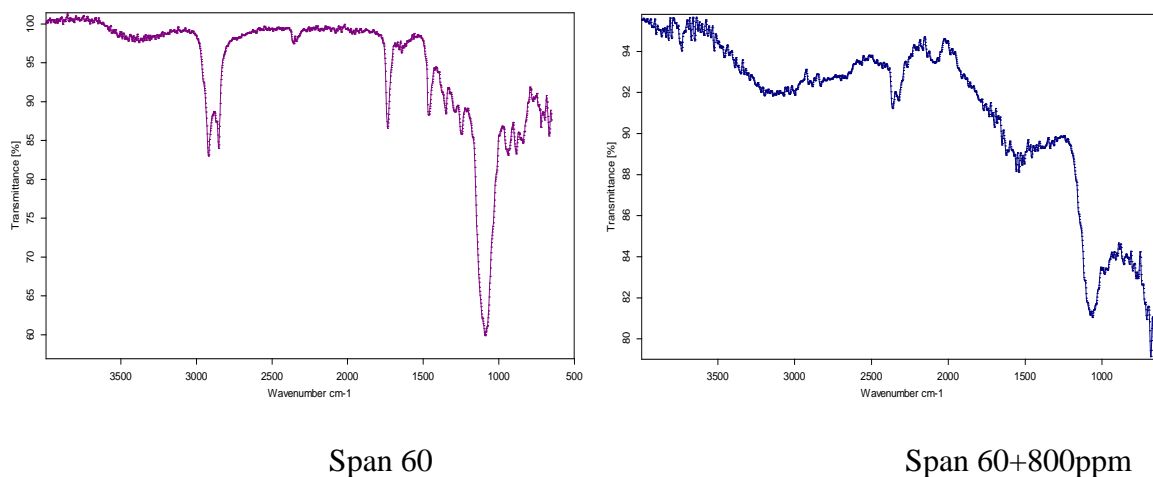


Figure 12. FT-IR transmittance spectrum of (a) Span 60 and (b) OL37+800 ppm Span 60

From figure 12a and 12b it can be observed all significant peaks in pure Span 60 shown up in adsorption film onto the OL 37 surface. The peak at 3453 cm^{-1} demonstrates the existence of the O-H stretching. The presence of C=O and C-O- C stretching frequency is clearly presents in the domain 1736 and to 1118 cm^{-1} . The peaks appearing near 2919 , 2853 , 1362 cm^{-1} and 765 cm^{-1} corresponding to the aliphatic C-H stretching vibration of the CH_2 and CH_3 groups.

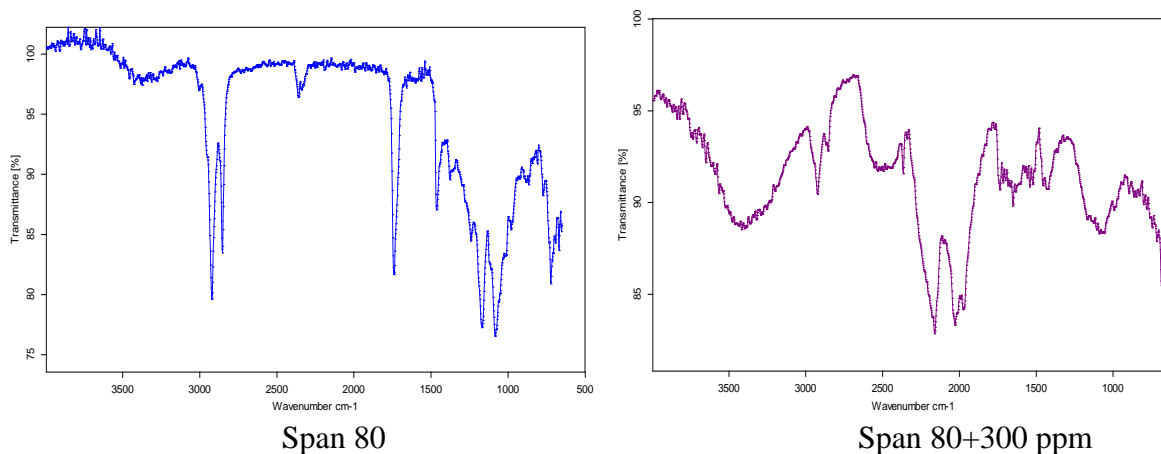


Figure 13. FT-IR transmittance spectrum of (a) Span 80 and (b) OL37+300 ppm Span 80

The spectrum of pure Span 80 is indicated in figure 13a. The peaks at 3459 cm^{-1} and 1642 are assigned OH group. It is be noted, that the absorption peaks at 1740 cm^{-1} , 1582 cm^{-1} 1377 cm^{-1} are ascribed to the C=O, C-H bending in CH_3 and CH_2

Figure 13b shows the FTIR spectra of the inhibitor adsorbed on the metal surface after immersion in $0.5\text{M H}_2\text{SO}_4$ solution with 300 ppm Span 80. It could be observed a band in the domain $3000\text{-}3500\text{ cm}^{-1}$ can be allocated of O-H group. The existence of C=O, C-O, C-H, CH_2 is verified by their stretching modes at 1738 cm^{-1} , 1169 cm^{-1} , 1357 cm^{-1} and $1082\text{-}722\text{ cm}^{-1}$ [2, 7, 35, 51-55].

Comparing figures 12a and 12b, 13a-13b, it can be suggested that Span 60 and Span 80 are adsorbed on the OL 37 surface.

3.6. Surface analysis by metallographic spectroscopy

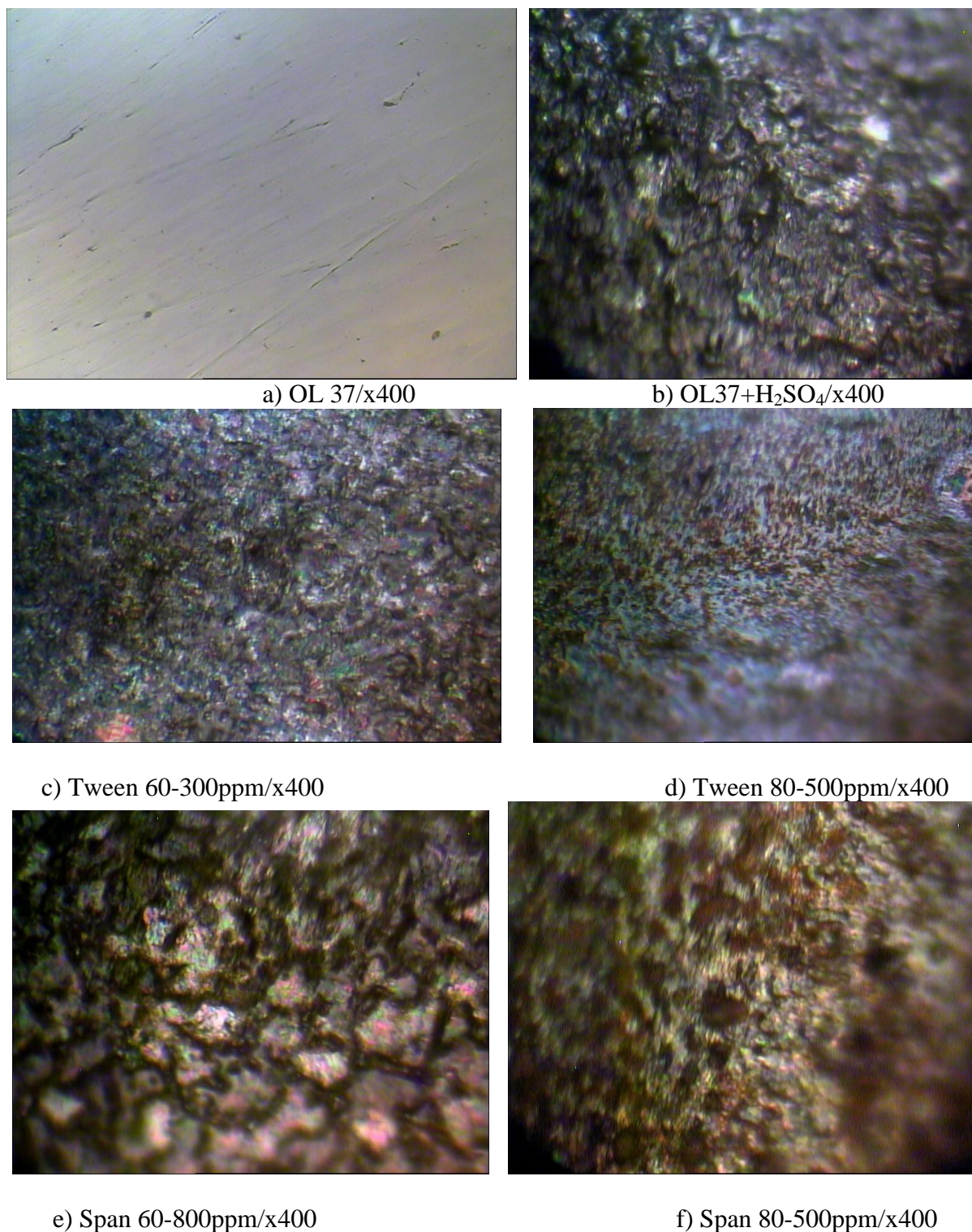


Figure 14. Micrographies of OL37 in 0.5M H₂SO₄ with and without of four nonionic surfactants as corrosion inhibitor at magnification X400

The obtaining of the protective surface layer of these nonionic surfactants on the electrode surface has been confirmed by metallurgical research microscope examination on the electrode surface.

Figure 14 presents certain micrographies were analyzed for our systems: Xppm Inhibitor/0.5M H₂SO₄/OL37. From figure 14 it can be observed some micrographies have been investigated for our systems: OL37 +H₂SO₄ before and after a certain period immersion in corrosive environment with and without of different concentrations of organic inhibitor of type Tween 60, Tween 80, Span 60 and Span 80 [2, 35, 52-55].

It can be established that the in the presence of organic inhibitors the surface becomes more smooth, uniform, compact and homogeneous than the uninhibited surface where indicating protective layers are obtained of adsorbed films of nonionic surfactants and corrosion products. In the presence of the inhibitor, the affecting of the carbon steel surfaces is importantly reduced; less corroded which demonstrates that the constitution of a protective layer onto the OL 37 surface has clear reduced the corrosion rate of the carbon steel. It can be established that these layers act as a barrier among aggressive environment and carbon steel surface and as a result the corrosion process is protected [2, 35, 51-55]

4. CONCLUSIONS

All the studied of these nonionic surfactants (Tween 60, Tween 80, Span 60 and Span 80) revealed a very good protection properties for the corrosion OL37 carbon steel in 0.5M H₂SO₄ and the corrosion current density decreased and the inhibitor effectiveness increased with increasing inhibitors concentrations.

The adsorption of all nonionic surfactants studied onto the OL 37 electrode in according the Langmuir adsorption isotherm model.

The results of FTIR, also reported the adsorption of inhibitor molecule on the electrode surface and blocking the active sites.

The EIS of OL 37 increases due to increasing the surface coverage of nonionic surfactant molecules onto the electrode surface, which determines in an increase in the inhibition effect.

Characterization and surface analysis by FTIR and metallographic spectroscopy demonstrate the formation of a protective layer onto the OL 37 surface and show the adsorption mechanism of all nonionic surfactants onto OL 37 surface in 0.5M H₂SO₄ medium.

Tween 60, Tween 80, Span 60 and Span 80 reacted as mixed type corrosion inhibitor.

In the present study, the inhibitors type Tween 60 and Tween 80 has an excellent efficiency; and Span 60 and Span 80 have a good efficiency.

The inhibition efficiency follows the order: Tween 60 > Tween 80 > Span 80 > Span 60 because the presence of these inhibitors causes a significant decrease in corrosion rate.

References

1. D. Jones, "Principle and Prevention of Corrosion", MacMillan Publishing Company, New York, 1992.
2. F. Branzoi and V. Branzoi, "Development in corrosion protection" Chapter 21, Edited by M. Aliofkhazraei, *INTECH*, 2014
3. V. Branzoi and F. Branzoi, *Rev. Roum. Chim.*, 47 (2002) 1193.
4. E. E. Oguzie, Y. Li and F. H. Wang, *J. Colloid. Interface Sc.*, 310 (2007) 90.
5. E. M. Sherif, A. A. Almajid, A. K. Bairamov and E. Al-Zahrani, *Int. J. Electrochem. Sci.*, 6 (2011) 5372.
6. V. Branzoi, F. Branzoi and M. Baibarac, *Mat. Chem. Phys.*, 65 (2000) 288.
7. F. Branzoi and V. Branzoi, *Int. J. Electrochem. Sci.*, 11 (2016) 6564.
8. M. El Azhar, B. Mernari, M. Traisnel, F. Bentiss and M. Lagrenee, *Corros. Sci.*, 43 (2001) 2229.
9. P. C. Okafar and Y. Zheng, *Corros. Sci.*, 51 (2009) 850.
10. C. Jeyaprabha, S. Sathiyarayanan and G. Venkatachari, *Electrochim. Acta*, 51 (2006) 4080.
11. A. K. Singh and M. A. Quraishi, *Corros. Sci.*, 52 (2010) 1373.
12. J. Wang and S. A. Xu, *Int. J. Electrochem. Sci.*, 11 (2016) 2621.
13. R. Solmaz, *Corros. Sci.*, 81 (2014) 75.
14. X. H. Li, S. D. Deng, X. G. Xie and H. Fu, *Corros. Sci.*, 56 (2014) 15.
15. D. Daoud, T. Douadi, H. Hamani, S. Chafaa and M. Al-Noaimi, *Corros. Sci.*, 94 (2015) 21.
16. B. Xie, S. S. Zhu, Y. L. Li, C. Lai, X. Lin, L. K. Zou, L. X. He and N. Chen, *J. Chinese Soc. Corros. Prot.*, 34 (2014) 365.
17. M. A. Hegazy, A. S. El-Tabei, A. H. Bedair and M. A. Sadeq, *Corros. Sci.*, 60 (2012) 219.
18. G. M. Al-Senani, *Int. J. Electrochem. Sci.*, 11 (2016) 291.
19. N. A. Negm, N. A. Kandile, E. A. Bahr and M. A. Mohamed, *Corros. Sci.*, 65 (2012) 95.
20. M. Lagrenee, B. Mernari, M. Bouanis, M. Traisnel and F. Bentiss, *Corros. Sci.*, 44 (2002) 573.
21. M. A. Hegazy, A. S. El-Tabei and H. M. Ahmed, *Corros. Sci.*, 54 (2012) 115.
22. J. Zhang, X. L. Gong, H. H. Yu and M. Du, *Corros. Sci.*, 53 (2011) 3324.
23. D. Gopi, K. M. Govindaraju and L. Cavitha *J. Appl. Electrochem.*, 40 (2010) 1349.
24. X. Tang, W. Yang, Y. Chen and R. Wana, *Corros. Sci.*, 52 (2010) 242.
25. P. Lowmunkhong, D. Ungthararak and P. Sutthivaiyakit, *Corros. Sci.*, 52 (2010) 30.
26. R. Hasanov, S. Bilge, S. Bilgic, G. Gece and Z. Kılıc, *Corros. Sci.*, 52 (2010) 984.
27. E. S. Meresht, T. S. Farahani and J. Neshati, *Corros. Sci.*, 54 (2012) 36.
28. M. A. Quraishi, A. Singh, V. K. Singh, D. K. Yadav and A. K. Singh, *Mater. Chem. Phys.*, 122 (2010) 1220.
29. Y. Yan, W. Li, L. Cai and B. Hou, *Electrochim. Acta*, 53 (2008) 5953.
30. S. Issaadi, T. Douadi, A. Zouaoui, S. Chafaa, M. A. Khan and G. Bouet, *Corros. Sci.*, 53 (2011) 1484.
31. A. M. Atta, O. E. El-Azabawy, H. S. Ismail and M. A. Hegazy, *Corros. Sci.*, 53 (2011) 1680.
32. A. Doner, R. Solmaz, M. Ozcan and G. Kardas, *Corros. Sci.*, 53 (2011) 2902.
33. X. Li, S. Deng and H. Fu, *Corros. Sci.*, 53 (2011) 3241.
34. A. K. Singh, A. K. Singh and E. E. Ebenso, *Int. J. Electrochem. Sci.*, 9 (2014) 352.
35. F. Branzoi, V. Branzoi and C. Licu, *Mater. Corros.*, 65 (2014) 637.
36. B. A. Abd-El-Naby, O. A. Abdullatef, E. Khamis and W. A. El-Mahmody, *Int. J. Electrochem. Sci.*, 11 (2016) 1271.
37. H.-H. Li, S.-D. Deng, H. Fu and G.-N. Mu, *J. Appl. Electrochem.*, 39 (2009) 1125.
38. M. A. Migahed, A. A. Farag, S. M. Elsaed, R. Kamal, M. Mostfa and H. Abd El-Bary, *Mater. Chem. Phys.*, 125 (2011) 125.
39. Q. Zhang, Z. Gao, X. Feng and X. Zou, *Colloids. Surf. A*, 380 (2011) 191.
40. D. Asefi, N. M. Mahmoodi and M. Arami, *Colloids. Surf. A*, 355 (2010) 183.

41. M. A. Migahed, H. M. Mohamed and A. M. Al-Sabagh, *Mater. Chem. Phys.*, 80 (2003) 169.
42. E. E. Oguzie, Y. Li and P. H. Wang, *Electrochim. Acta*, 53 (2007) 909.
43. S. S. Abdel Rehim, O. A. Hazzazi, M. A. Amin and K. F. Khaled, *Corros. Sci.*, 50 (2008) 2258.
44. A. K. Singh and M. A. Quraishi, *J. Appl. Electrochem.*, 40 (2010) 1293.
45. R. Solmaz, G. Kardas, M. Culha and M. Erbil, *Electrochim. Acta*, 53 (2008) 5941.
46. E. A. Noor and A. H. Al-Maubaraki, *Mat. Chem. Phys.*, 110 (2008) 145
47. L. Larabi, O. Benali and Y. Harek, *Mater. Lett.*, 61 (2007) 3287.
48. M. Lebrini, F. Bentis, H. Vezin and M. Lagrene, *Corros. Sci.*, 48 (2006) 1279.
49. S. M. A. Hosseini and A. Azimi, *Mater. Corros.*, 59 (2008) 41.
50. A. Popova, E. Sokolova, S. Raicheva and M. Christov, *Corros. Sci.*, 45 (2003) 33.
51. F. Bontiss, M. Lagrence and M. Traisnel, *Corrosion*, 56 (2000) 733.
52. Y. Okada, K. Tanaka, E. Sato and H. Okajima, *Org. Biomol. Chem.*, 4 (2006) 4113.
53. Q. Qu, S. A. Jiang, W. Bai and L. Li, *Electrochim. Acta*, 52 (2007) 6811.
54. M. J. Bahrami, S. M. A. Hosseini and P. Pilvar, *Corros. Sci.*, 52 (2010) 2793.
55. M. F. L. Granero, P. H. L. S. Matai, I. V. Aoki and I. C. Guedes, *J. Appl. Electrochem.*, 39 (2009) 1199.

© 2017 The Authors. Published by ESG (www.electrochemsci.org). This article is an open access article distributed under the terms and conditions of the Creative Commons Attribution license (<http://creativecommons.org/licenses/by/4.0/>).